J. Biochem. **141**, 57–68 (2007)
doi:10.1093/jb/mvm011

Tetraplex Structure of Fission Yeast Telomeric DNA and Unfolding of the Tetraplex on the Interaction with Telomeric DNA Binding Protein Pot1

Hidetaka Torigoe* and Ayako Furukawa

Department of Applied Chemistry, Faculty of Science, Tokyo University of Science, 1-3 Kagurazaka, Shinjuku-ku, Tokyo 162-8601, Japan

Received September 12, 2006; accepted November 13, 2006; published online December 11, 2006

To understand the regulation mechanism of fission yeast telomeric DNA, we analysed the structural properties of Gn: d(G_nTTAC) ($n = 2–6$) and 4Gn: d(G_nTTAC)$_4$ ($n = 3$ and 4), and their interaction with the single-stranded telomeric DNA binding domain of telomere-binding protein Pot1 (Pot1DBD). G4, G5 and G6 formed a parallel tetraplex in contrast with no tetraplex formation by G2 and G3. Also, 4G4 adopted only an antiparallel tetraplex in spite of a mixture of parallel and antiparallel tetraplexes of 4G3. The variety of tetraplex structures was governed by the number of consecutive guanines in a single copy and the number of repeats. The antiparallel tetraplex of 4G4 became unfolded upon the interaction with Pot1DBD. The interaction with mutant Pot1DBD proteins revealed that the ability to unfold the antiparallel tetraplex was strongly correlated with the specific binding affinity for the single-stranded telomeric DNA. The result suggests that the decrease in the free single strand upon the complex formation with Pot1DBD may shift the equilibrium from the tetraplex to the single strand, which may cause the tetraplex unfolding. Considering that the antiparallel tetraplex inhibits telomerase-mediated telomere elongation, we conclude that the ability of Pot1 to unfold the antiparallel tetraplex is required for telomerase-mediated telomere regulation.

Key words: CD spectroscopy, fluorescence resonance energy transfer, telomeric DNA, telomeric DNA binding protein, tetraplex.

Abbreviations: EMSA, electrophoretic mobility shift assay; Fam, 6-carboxyfluorescein; FRET, fluorescence resonance energy transfer; GST, glutathione S-transferase; IPTG, isopropyl-β-D-thiogalactopyranoside; ITC, isothermal titration calorimetry; Pot1DBD, single-stranded telomeric DNA binding domain of fission yeast telomere-binding protein Pot1; WT, wild-type Pot1DBD.

The telomere is the nucleoprotein complex located at the ends of linear eukaryotic chromosomes (*1–5*). It is essential for maintaining chromosomal stability to inhibit DNA degradation, preventing fusion between chromosomes, and achieving accurate and complete replication of the chromosomal ends (*1–5*). Telomeric DNA consists of tandemly repeated sequences, one strand being rich in guanines. The G-rich strand terminates with a single-stranded 3′ overhang. The telomeric DNA sequences are either composed of perfect repeats, such as d(T_2G_4) in *Tetrahymena* (*6*), d(T_4G_4) in *Oxytricha* and *Stylonychia* (*7, 8*), and d(T_2AG_3) in more than 100 vertebrates including human (*9*), or show some sequence heterogeneity, for example d($G_{1-3}T$) in *Saccharomyces cerevisiae* (*10*) and d($G_{1-8}TTACA_{0-1}C_{0-1}$) in *Schizosaccharomyces pombe* (*11, 12*). The length of telomeric DNA decreases with cell age, and when the telomeric DNA is significantly degraded, the cell dies (*13–16*). It has been suggested that immortalized cells have sufficient telomerase activity to preserve their telomeric DNA indefinitely, and that this activity is important for maintaining the immortalized state (*1–5*). This possible relation to cell aging and cancer has recently led to considerable interest in the G-cluster telomeric DNA.

The G-cluster telomeric DNA sequences have the ability to form defined tetraplex structures (*17–19*). The fundamental structural unit of the tetraplex structure is composed of four guanine residues aligned with each other in a square planar configuration (*17–21*). Each guanine interacts with each of the two adjacent guanines through two non-Watson–Crick G•G base pair hydrogen bonds (*17–21*). The tetraplex structures of G-cluster sequences can be formed tetramolecularly via the parallel alignment of four strands (*22*), bimolecularly via the association of two hairpins (*23*) or monomolecularly via intramolecular folding (*24*), and are stabilized by cations such as Na^+ or K^+ (*24*). Although the tetraplex structures of the perfectly repetitive telomeric DNA sequences from *Tetrahymena* (*23–27*), *Oxytricha* (*24, 26*), and vertebrates (*27–30*) have been well-characterized, few studies have been reported on the tetraplex formation by the irregularly repetitive telomeric DNA sequences from budding and fission yeasts.

The biological role of the tetraplex structure formation remains unknown. Nevertheless, evidence has been obtained, suggesting that the tetraplex structure may

*To whom correspondence should be addressed: Tel: 81-3-5228-8259, Fax: 81-3-5261-4631, E-mail: htorigoe@ch.kagu.tus.ac.jp

exist *in vivo* (*17, 19, 31*). Tetraplex DNA-binding proteins have been identified in several organisms (*32–39*), and some DNA-binding proteins have the ability to unfold the tetraplex structure (*40–46*), although the biological role of these proteins needs to be established. No fission yeast proteins have been reported to bind with or unfold the tetraplex structure.

Fission yeast Pot1 is a single-stranded telomeric DNA-binding protein (*47*). The N-terminal region of fission yeast Pot1 ranging from amino acids 1–185 is a single-stranded telomeric DNA-binding domain (Pot1DBD) (*12, 48, 49*). A six-base single-stranded DNA, d(GGTTAC), is the minimum telomeric DNA sequence for the specific binding of Pot1DBD (*12, 48, 49*). Previous studies revealed that overexpression of fission yeast Pot1 led to modest but significant telomere lengthening *in vivo* (*12, 50*). On the other hand, tetraplex formation is known to inhibit the telomerase-mediated telomere elongation (*51–53*). We hypothesize that Pot1DBD may promote telomerase-mediated telomere elongation by unfolding the tetraplex, if the fission yeast telomeric DNA forms the tetraplex. The possibility should be examined to discuss the biological role of fission yeast Pot1 *in vivo*.

In the present study, we analysed the structural properties of a series of fission yeast telomeric DNA sequences, Gn: $d(G_nTTAC)$ ($n = 2$–6) and 4Gn: $d(G_nTTAC)_4$ ($n = 3$ and 4), to reveal the tetraplex formation ability of the fission yeast telomeric DNA with some sequence heterogeneity *in vivo*. We have found that the telomeric DNA sequences with more consecutive G bases (G4, G5, G6, 4G3 and 4G4) in the presence of the sodium cation formed a tetraplex structure with different folding topology. The tetraplex topology of the irregularly repetitive telomeric DNA from fission yeast was governed by the number of consecutive guanines in a single copy and the number of repeats similar to that of the perfectly repetitive telomeric DNAs from *Tetrahymena*, *Oxytricha* and vertebrates. We further examined the interaction of the tetraplex structure with the wild-type or a series of mutant Pot1DBD proteins. We have demonstrated that the tetraplex structure became unfolded upon the interaction with Pot1DBD. The study of the interaction with a series of mutant Pot1DBD proteins revealed that the ability to unfold the tetraplex was strongly correlated with the specific binding affinity for the single-stranded DNA. On the basis of these results, the mechanism and the biological role of the unfolding ability of Pot1DBD will be discussed.

MATERIALS AND METHODS

Preparation of Oligonucleotides—The oligonucleotides used in this study are listed in Table 1. Crude oligonucleotides of a series of telomeric DNAs, Gn: $d(G_nTTAC)$ ($n = 2$–6) and 4Gn: $d(G_nTTAC)_4$ ($n = 3$ and 4), and ones of control nontelomeric DNAs, Tn: dT_n ($n = 28$ and 32) were purchased from Nisshinbo Corp. (Japan), and purified by a reverse-phase HPLC on a Wakosil DNA column by the standard procedure. Purified dye-labelled oligonucleotides, F4G4D: Fam-$d(G_4TTAC)_4$-Dabcyl and FT32D: Fam-dT_{32}-Dabcyl [where 6-carboxyfluorescein (Fam) is a fluorophore and Dabcyl is a quencher], were purchased from Thermo Electron Corp. (Germany). The purified oligonucleotide solutions in the experimental buffer were heated at 95°C for 10 min, followed by gradual cooling to room temperature, and were then kept at room temperature for at least 2 days before the experiments. The concentrations of the oligonucleotide solutions were determined from the absorbance at 260 nm.

Table 1. **Oligonucleotide DNA sequences used in this study.**

Name	DNA sequence
G2	5′-d(GGTTAC)-3′
G3	5′-d(GGGTTAC)-3′
G4	5′-d(GGGGTTAC)-3′
G5	5′-d(GGGGGTTAC)-3′
G6	5′-d(GGGGGGTTAC)-3′
4G3	5′-$d(GGGTTAC)_4$-3′
4G4	5′-$d(GGGGTTAC)_4$-3′
T28	5′-dT_{28}-3′
T32	5′-dT_{32}-3′
F4G4D	5′-Fam-$d(GGGGTTAC)_4$-Dabcyl-3′
FT32D	5′-Fam-dT_{32}-Dabcyl-3′

Fam, 6-carboxyfluorescein.

Preparation of Wild-type and Mutant Pot1DBD Proteins—The gene fragment coding for Pot1DBD was cloned into the EcoRI and SmaI sites of an *Escherichia coli* expression vector, pGEX6P-1 (Amersham Biosciences), fused with the glutathione S-transferase (GST) gene. The expression plasmid was transferred into *E. coli* BL21 cells. Cells were grown in LB medium containing ampicillin (50 mg/l) at 25°C, up to an OD_{600} of 1.0. Production of the protein was induced by the addition of isopropyl-β-D-thiogalactopyranoside (IPTG) to 0.4 mM, and the cells were grown for an additional 5 h. The cells were harvested by centrifugation, and suspended in BugBuster Protein Extraction Reagent (Novagen) containing Benzonase Nuclease (Novagen). After incubation for 20 min at room temperature, cell debris was removed by centrifugation. The supernatant containing the GST-Pot1DBD fusion protein was first purified by Glutathione Sepharose 4B affinity open column (Amersham Bioscience). PreScission Protease (Amersham Biosciences) was added to remove the GST tag. The Pot1DBD protein was further purified on a HiPrep 16/10 CM Sepharose Fast Flow column (Amersham Bioscience) with AKTA purifier system (Amersham Bioscience). The protein at this stage was >99% pure, and the N-terminal amino acid sequence and molecular weight of the final product of the Pot1DBD protein were confirmed by amino acid sequencing and mass spectrometry, respectively. Site-directed mutations were introduced into the gene coding for Pot1DBD using suitable primers and a QuikChange site-directed mutagenesis kit (Stratagene). The presence of the desired mutations was confirmed by DNA sequencing of the gene constructs. Mutant Pot1DBD proteins were prepared in the same way as the wild-type Pot1DBD protein described earlier.

Electrophoretic Mobility Shift Assay (EMSA)—Oligonucleotides were labelled with [γ-^{32}P] ATP (6000 Ci/mmol, Amersham Biosciences) using T4 polynucleotide kinase (Toyobo). The ^{32}P–labelled oligonucleotides of Gn ($n = 2$–6) were mixed with the corresponding unlabelled oligonucleotides to achieve a final concentration of 5 μM, heated at 95°C for 10 min, followed by gradual cooling to room temperature, and were then kept at room temperature for at least two days. To analyse the interaction with the wild-type or mutant Pot1DBD, the protein was mixed with the ^{32}P–labelled oligonucleotides, and then incubated at 25°C for 30 min. Then, only the oligonucleotides or the interaction mixture was loaded on a 10 or 15% nondenaturing polyacrylamide gel. Electrophoresis was carried out in 0.5 × TBE at 10 V/cm and 4°C for 5 h.

CD Spectroscopy—CD spectra (*25, 26*) of the DNA and DNA-protein complexes in buffer A (20 mM Tris–HCl and 1 mM DTT) containing 150 mM NaCl at 25°C were recorded on a Jasco J-725 spectropolarimeter interfaced with a microcomputer. The cell path length was 1 cm. The scanning speed was 50 nm/min, and each spectrum was the average of subsequent eight scans. The DNA concentration was 5 μM for Gn ($n = 2$–6) and 3 μM for 4Gn ($n = 3$ and 4), T28 and T32, respectively. Either the wild-type or mutant Pot1DBD or GST was added step by step to each DNA sample in the indicated DNA/protein ratio, and the resulting complex was incubated at 25°C for 60 min before the measurements.

Fluorescence Resonance Energy Transfer (FRET) Analyses—FRET measurements (*54, 55*) in buffer A containing 150 mM NaCl at 25°C were carried out on a JASCO FP-6300 spectrofluorometer interfaced with a microcomputer. A 1 cm × 1 cm quartz cuvette was used. For emission spectra, the excitation wavelength was set at the wavelength where the absorption of the donor, 6-carboxyfluorescein, was maximal (495 nm). The DNA concentration was 100 nM for F4G4D and FT32D. Either the wild-type or mutant Pot1DBD was added step by step to each DNA sample in the indicated DNA/protein ratio, and the resulting complex was incubated at 25°C for 60 min before the measurements.

RESULTS

Electrophoretic Mobility Analyses of a Series of Fission Yeast Telomeric DNA Sequences—The electrophoretic mobilities of a series of fission yeast telomeric DNA sequences (Table 1), Gn: d(G_nTTAC) ($n = 2$–6) and 4Gn: d(G_nTTAC)$_4$ ($n = 3$ and 4), and control nontelomeric DNA sequences (Table 1), Tn: dT_n ($n = 28$ and 32), at pH 7.5 in buffer A (20 mM Tris-HCl and 1 mM DTT) containing 150 mM NaCl were analysed on a 15% nondenaturing polyacrylamide gel (Fig. 1). Figure 1A shows that G2 and G3 each migrated as a single band corresponding to a single-stranded structure. In contrast, G4, G5 and G6 each migrated as two distinct bands exhibiting different electrophoretic mobilities. The faster migrating band is assigned to a single-stranded structure, but the slower migrating one likely corresponds to an intermolecular polymeric structure with an apparently high molecular weight. This indicates that a part of each of

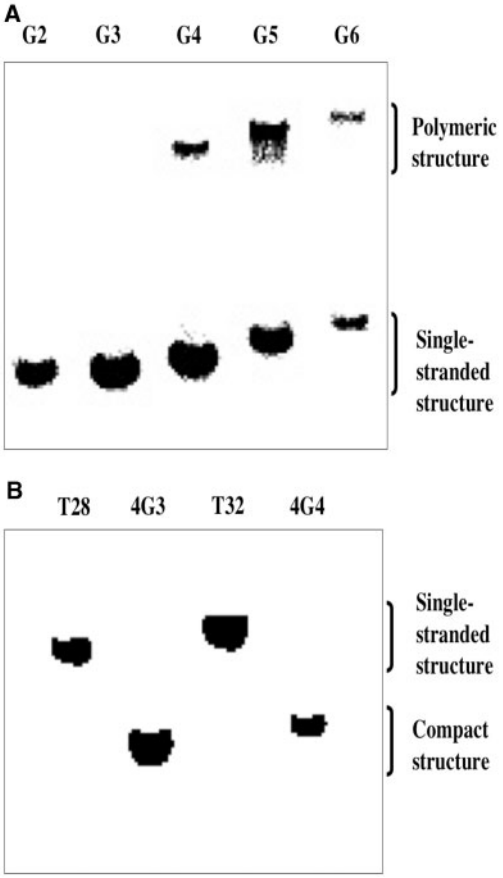

Fig. 1. **Electrophoretic mobility of Gn ($n = 2$–6) (A), 4Gn ($n = 3$ and 4) (B), and Tn ($n = 28$ and 32) (B) on a 15% nondenaturing polyacrylamide gel**. The ^{32}P-labelled DNA samples were prepared at pH 7.5 in buffer A (see 'Materials and Methods') containing 150 mM NaCl. The DNA concentrations in (A) and (B) were 5 μM and 200 μM, respectively. The gels were run in 0.5 × TBE at 10 V/cm and 4°C for 5 h.

G4, G5 and G6 forms an intermolecular polymeric structure. Figure 1B shows that, regardless of having the same number of base pairs, 4G3 migrated faster than T28, and 4G4 exhibited enhanced electrophoretic mobility compared to T32. The higher mobilities of 4G3 and 4G4 indicate that 4G3 and 4G4 form more compact structures than T28 and T32, respectively, which presumably involves intramolecular folding.

CD Spectroscopy of a Series of Fission Yeast Telomeric DNA Sequences—To reveal the conformational properties of the intermolecular polymeric structures of G4, G5 and G6, and those of the more compact structures of 4G3 and 4G4 (Fig. 1), we measured CD spectra of Gn ($n = 2$–6) (Fig. 2A) and 4Gn ($n = 3$ and 4) (Fig. 2B) at 25°C and pH 7.5 in buffer A containing 150 mM NaCl. The CD spectrum of G2 exhibits a positive peak at 276 nm and a negative one around 250 nm. This type of spectrum is typical of unstructured single-stranded DNA (*25, 26*). The CD spectrum pattern of G3 is similar to that of G2, although the ellipticity at 260 nm is increased. These CD spectra indicate that G2 and G3 form an unstructured single-strand, which is consistent

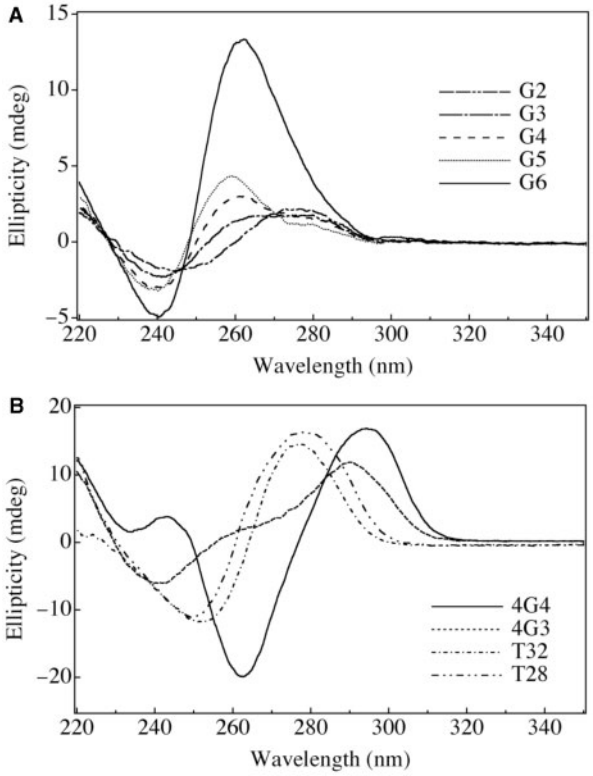

Fig. 2. **CD spectra of Gn ($n = 2$–6) (A), 4Gn ($n = 3$ and 4) (B) and Tn ($n = 28$ and 32) (B) at 25°C and pH 7.5 in buffer A (see 'Materials and Methods') containing 150 mM NaCl**. The DNA samples were prepared as described under 'Materials and Methods'. The DNA concentrations in (A) and (B) were 5 μM and 3 μM, respectively.

with the results of the electrophoretic mobility analyses in Fig. 1A. On the other hand, the CD spectra of G4 and G5 exhibit a positive peak at 260 nm and a negative one at 240 nm. This type of spectrum is typical of a parallel tetraplex DNA consisting of a parallel four-stranded tetrameric structure (*25, 26*). The CD spectrum of G6 shows the highest positive peak at 260 nm and the lowest negative one at 240 nm among the five examined oligonucleotides, which is the most typical CD pattern of parallel tetraplex DNA (*25, 26*). These results indicate that G4, G5 and G6 have the ability to form the parallel tetraplex DNA under the present experimental conditions with 150 mM sodium cation. The slower migrating band of each of G4, G5 and G6 observed in Fig. 1A corresponds to the parallel tetraplex DNA.

The CD spectra of both T32 and T28 exhibit a positive peak at 276 nm and a negative one at 250 nm, which is typical of unstructured single-stranded DNA. This result shows that neither T32 nor T28 forms any higher-order structure under the present experimental conditions. On the other hand, the CD spectrum of 4G4 exhibits a positive peak at 295 nm and a negative one at 264 nm. This type of spectrum is typical of an antiparallel tetraplex DNA consisting of an intramolecular antiparallel four-stranded structure (*25, 26*), indicating that 4G4 forms intramolecular antiparallel tetraplex DNA under the present experimental conditions with 150 mM sodium cation. In the CD spectrum of 4G3, a small positive peak around 260 nm and a negative one at 240 nm appear in addition to a large positive peak near 290 nm corresponding to an antiparallel tetraplex DNA. As in the cases of G4, G5 and G6, the positive peak around 260 nm and the negative one at 240 nm are ascribed to a parallel tetraplex DNA (*25, 26*). Thus, the conformation of 4G3 is a mixture of parallel and antiparallel tetraplex DNA, although the electrophoretic mobility of the two species may be almost identical (Fig. 1B). These results indicate that 4G3 and 4G4 have the ability to form parallel or antiparallel tetraplex DNA under the present experimental conditions with 150 mM sodium cation. The faster migration bands of 4G3 and 4G4 relative to those of T28 and T32, respectively, observed in Fig. 1B correspond to the parallel or antiparallel tetraplex DNA, which may be more compact than unstructured single-stranded DNA.

EMSA of the Interaction between the Fission Yeast Telomeric DNAs and Pot1DBD—The interaction between Pot1DBD and each of the fission yeast telomeric DNAs (G2, G6, T32 and 4G4) at pH 7.5 in buffer A with or without 150 mM NaCl was analysed on a 10% or 15% nondenaturing polyacrylamide gel by EMSA (Fig. 3). G2 was the unstructured single strand in both the absence and presence of 150 mM sodium cation (G2 in Fig. 1a, and lanes 1 and 2 in Fig. 3A). When Pot1DBD was added, Pot1DBD was able to interact with G2 (lane 3 in Fig. 3A), which is consistent with the previously reported finding that G2 is the minimum telomeric DNA sequence for the specific binding of Pot1DBD (*12, 48, 49*). On the other hand, the addition of the sodium cation induced the formation of the parallel tetraplex DNA of G6 (G6 in Fig. 1A, and lanes 4 and 5 in Fig. 3A). Pot1DBD was capable of interacting with both the unstructured single strand and the parallel tetraplex of G6 (lane 6 in Fig. 3A). The interaction of Pot1DBD with the unstructured single strand of G6 is quite reasonable, because the DNA sequence of G6 contains the minimum DNA sequence, d(GGTTAC), for the specific binding of Pot1DBD (*12, 48, 49*). These results indicate that Pot1DBD has the ability to interact with parallel tetraplex DNA as well as unstructured single strand DNA. In contrast, Pot1DBD was unable to interact with the unstructured single strand of T32 (T32 in Fig. 1B, and lanes 1 and 2 in Fig. 3B), which does not contain the minimum DNA sequence, d(GGTTAC), for the specific binding of Pot1DBD. On the other hand, Pot1DBD was able to interact with the antiparallel tetraplex of 4G4 (4G4 in Fig. 1B, and lanes 3 and 4 in Fig. 3B). Overall, we have concluded that Pot1DBD is capable of interacting with both parallel and antiparallel tetraplex DNA.

CD Spectroscopy of the Interaction between the Fission Yeast Telomeric DNAs and Pot1DBD—The CD spectral change of G2 upon the addition of Pot1DBD was measured at 25°C and pH 7.5 in buffer A containing 150 mM NaCl (Fig. 4A). An increase in the ellipticity in the range of 240–260 nm and a decrease in that in the range of 260–290 nm were observed upon the addition of Pot1DBD. On the basis of the previously reported X-ray

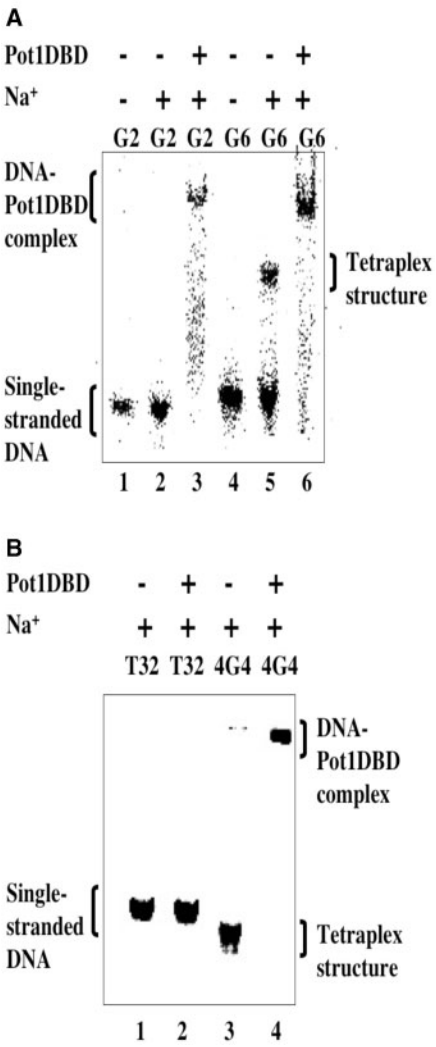

Fig. 3. **EMSA for the complex formation between Pot1DBD and each of G2, G6, T32, and 4G4 on a non-denaturing polyacrylamide gel**. (A) ^{32}P-labelled G2 and G6 were prepared at pH 7.5 in buffer A (see 'Materials and Methods') without (lanes 1 and 4) or with (lanes 2 and 5) 150 mM NaCl. The ^{32}P-labelled G2 and G6 (500 nM) at pH 7.5 in buffer A containing 150 mM NaCl was incubated with Pot1DBD (12.4 μM) in the same buffer at 25°C for 30 min (lanes 3 and 6). The 10% nondenaturing gel was run in 0.5 × TBE at 10 V/cm and 4°C for 5 h. (B) ^{32}P-labelled T32 and 4G4 were prepared at pH 7.5 in buffer A (see 'Materials and Methods') containing 150 mM NaCl (lanes 1 and 3). The ^{32}P-labelled T32 and 4G4 (20 nM) at pH 7.5 in buffer A containing 150 mM NaCl were incubated with Pot1DBD (3.2 μM) in the same buffer at 25°C for 30 min (lanes 2 and 4). The 15% nondenaturing gel was run in 0.5 × TBE at 10 V/cm and 4°C for 5 h.

crystallographic structure of the complex between G2 and Pot1DBD (*49*), these changes in ellipticity may result from the highly compact, folded conformation of G2 upon the complex formation with Pot1DBD. However, the details of the structural distortion causing these changes in ellipticity remain to be established.

To examine the properties of the interaction between Pot1DBD and the parallel tetraplex of G6 (lane 6 in Fig. 3A), the CD spectral change of G6 upon the addition of Pot1DBD was examined at 25°C and pH 7.5 in buffer A containing 150 mM NaCl (Fig. 4B). The addition of Pot1DBD to G6 decreases the ellipticity in the range of 260–290 nm. G6 forms both the unstructured single-strand and the parallel tetraplex under the present experimental conditions (lane 5 in Fig. 3A). Because the DNA sequence of G6 contains the minimum DNA sequence, d(GGTTAC), for the specific binding of Pot1DBD (*12, 48, 49*), the single-stranded component of G6 has the ability to bind with Pot1DBD, which may produce a CD spectral change similar to that observed for the Pot1DBD-G2 binding (Fig. 4A). Thus, the observed decrease in the ellipticity in the range of 260–290 nm (Fig. 4B) includes the effect of the CD spectral change for the binding between Pot1DBD and the single-stranded component of G6. Therefore, the change in the ellipticity at 260 nm for the binding between Pot1DBD and the parallel tetraplex component of G6 is not significant. This indicates that Pot1DBD does not appreciably decrease the amount of the parallel tetraplex of G6.

To examine the properties of the interaction between Pot1DBD and the antiparallel tetraplex of 4G4 (lane 4 in Fig. 3B), the CD spectral change of 4G4 upon the addition of Pot1DBD was measured at 25°C and pH 7.5 in buffer A containing 150 mM NaCl (Fig. 4C) or 30 mM KCl (Fig. 4D). Without Pot1DBD, 4G4 formed the antiparallel tetraplex both in the presence of sodium and potassium cation. The ellipticity of the positive peak at 295 nm was decreased upon the addition of Pot1DBD in a concentration-dependent manner both in the presence of sodium and potassium cation. The decrease in the ellipticity of the positive peak at 295 nm (Fig. 4C and D) was not obtained for the CD spectral change observed for the Pot1DBD-G2 binding (Fig. 4A). Thus, the decrease in the ellipticity at 295 nm corresponds not to the specific binding with Pot1DBD, but to the decrease in the amount of the antiparallel tetraplex on the interaction with Pot1DBD. In contrast, no significant change in the CD spectrum of 4G4 was observed upon the addition of GST (Fig. 4E). These results indicate that Pot1DBD has the ability to decrease the amount of the antiparallel tetraplex of 4G4, and the ability to reduce the amount of the antiparallel tetraplex is specific for Pot1DBD. Furthermore, the addition of Pot1DBD did not induce any significant change in the CD spectrum of T32 (Fig. 4F). This result is consistent with the inability of Pot1DBD to bind with T32 (lane 2 in Fig. 3B). This shows that Pot1DBD did not have any effect on the structure of the single-stranded DNA, which does not bind with Pot1DBD. Based on all the results in Fig. 4, we have concluded that the interaction with Pot1DBD decreases the amount of the antiparallel tetraplex DNA.

FRET Analysis of the Interaction between the Fission Yeast Telomeric DNAs and Pot1DBD—To reveal why the addition of Pot1DBD reduced the amount of the antiparallel tetraplex DNA (Fig. 4), the structural change of 4G4 upon the addition of Pot1DBD (Fig. 5A) was examined by FRET analysis (*54, 55*) at 25°C and

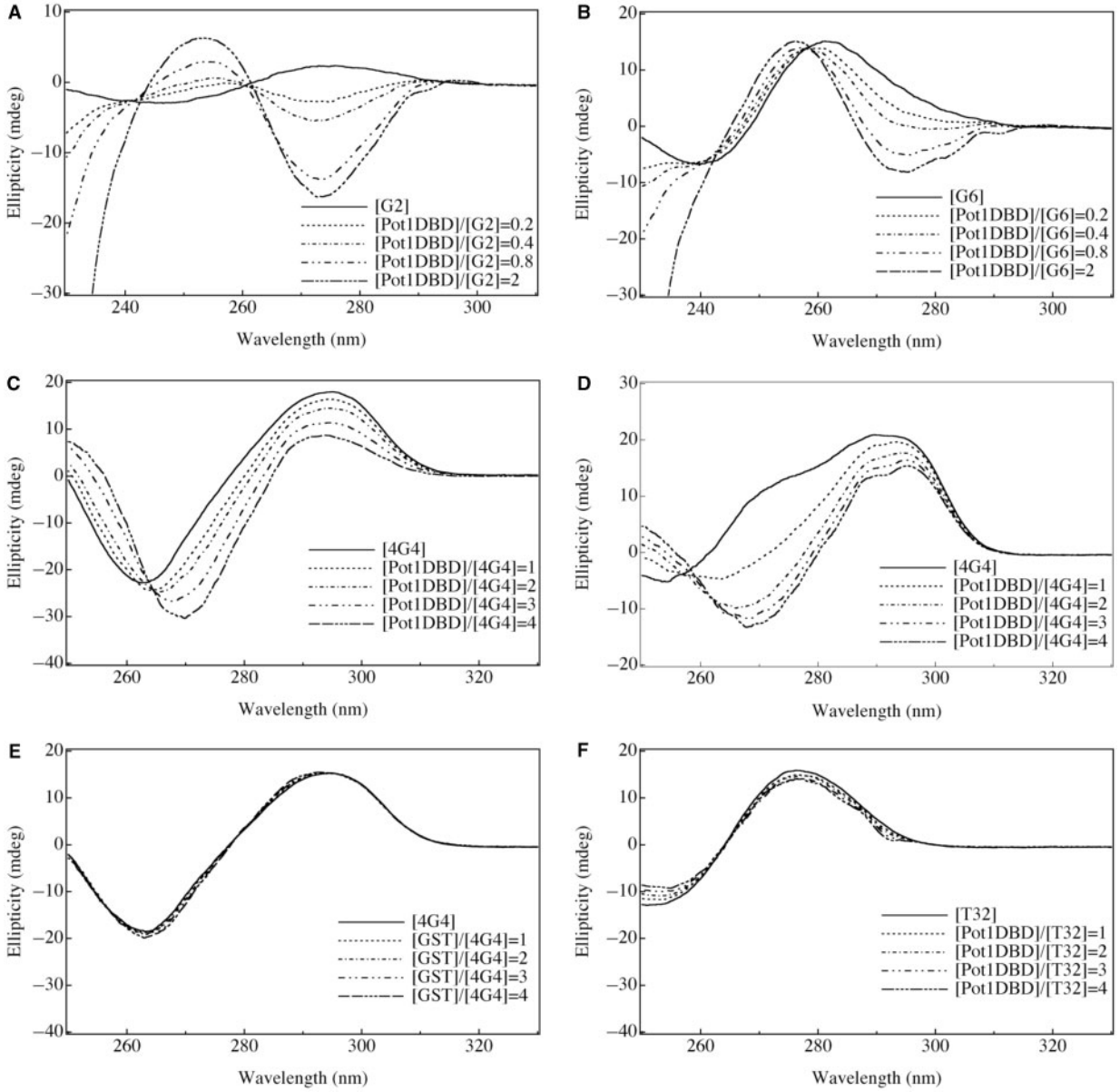

Fig. 4. **CD spectral changes upon the DNA–protein interaction.** The DNA at pH 7.5 in buffer A (see 'Materials and Methods') containing 150 mM NaCl (A–C, E, F) or 30 mM KCl (D) was incubated in the indicated molar ratio with the protein in the same buffer at 25°C for 60 min before the CD measurements. (A) 5 μM G2 titrated with Pot1DBD. (B) 5 μM G6 titrated with Pot1DBD. (C, D) 3 μM 4G4 titrated with Pot1DBD. (E) 3 μM 4G4 titrated with GST. (F) 3 μM T32 titrated with Pot1DBD.

pH 7.5 in buffer A containing 150 mM NaCl (Fig. 5B) or 30 mM KCl (Fig. 5C). The fluorophore, 6-Fam, and the quencher, dabcyl, were attached to the 5′ and 3′ termini of 4G4, respectively, to give the dual-labelled F4G4D (Table 1). Because the intramolecular folding of the antiparallel tetraplex structure of F4G4D in the presence of the sodium or potassium cation should bring the fluorophore and the quencher into close enough proximity for energy transfer, FRET-mediated quenching between the fluorophore and the quencher was observed (Fig. 5A). Thus, F4G4D showed low fluorescence due to FRET-mediated quenching. The addition of Pot1DBD enhanced the intensity of 6-Fam emission at 520 nm in a concentration-dependent manner both in the presence of the sodium and potassium cation (Fig. 5B and C). The increase in the fluorescence intensity corresponds to the increase in the distance between the fluorophore and the quencher, indicating unfolding of the antiparallel tetraplex structure of F4G4D. This result is consistent with the decrease in the amount of the antiparallel tetraplex of 4G4, observed as the CD spectral change upon the addition of Pot1DBD (Fig. 4C and D). Furthermore, dual-labelled FT32D (Table 1) was also prepared by attaching the fluorophore, 6-Fam, and the quencher, dabcyl, to the 5′ and 3′ termini of T32, respectively. The addition of Pot1DBD did not induce

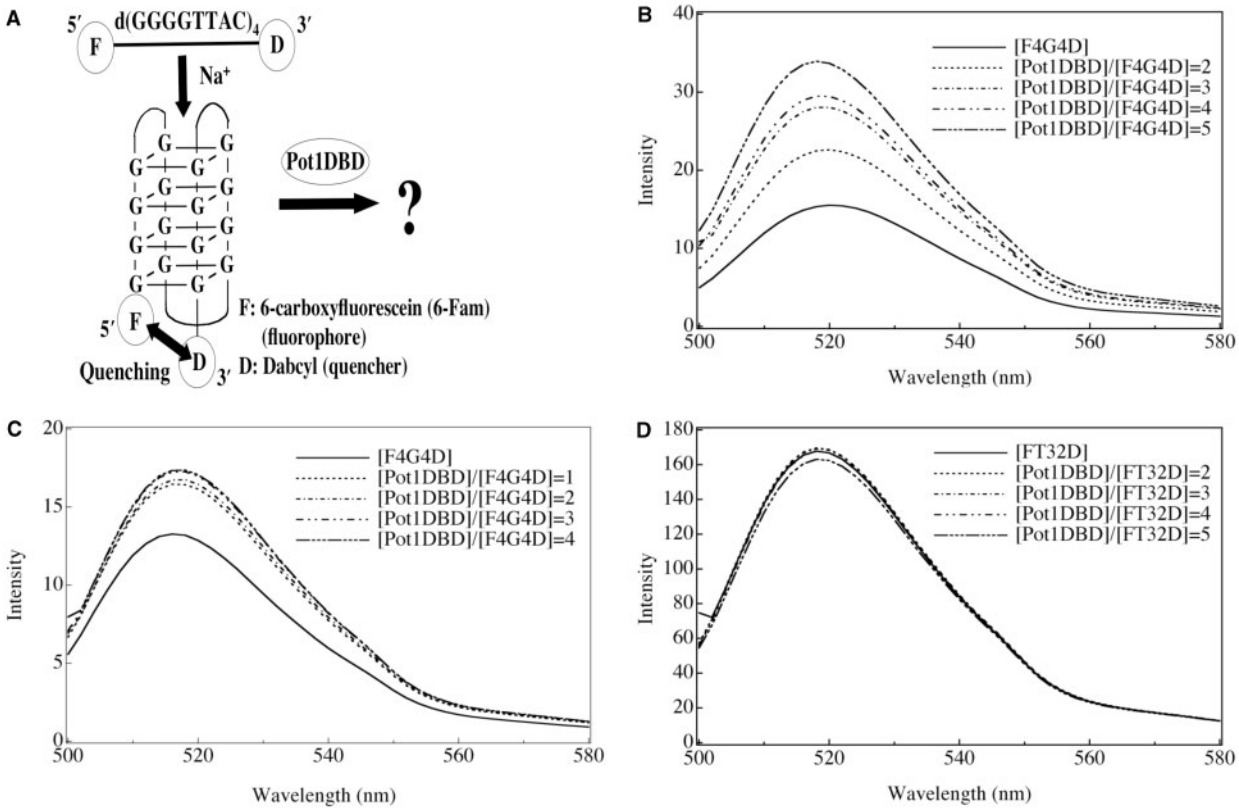

Fig. 5. **FRET analyses of the interaction with Pot1DBD**. (A) Experimental scheme for the FRET analyses. The exact structure of the antiparallel tetraplex of F4G4D is unknown. (B–D) 100 nM F4G4D (B, C) or 100 nM FT32D (D) at pH 7.5 in buffer A (see 'Materials and Methods') containing 150 mM NaCl (B, D) or 30 mM KCl (C) was incubated in the indicated molar ratio with Pot1DBD in the same buffer at 25°C for 60 min before the fluorescence measurements. The excitation wavelength was 495 nm.

any significant change in the fluorescence emission spectra of FT32D (Fig. 5D). This result is consistent with the inability of Pot1DBD to bind with T32 (lane 2 in Fig. 3B). This result shows that Pot1DBD did not cause any significant structural change of FT32D, which does not bind with Pot1DBD. Combining the results in Fig. 5, we have concluded that Pot1DBD has the ability to unfold the antiparallel tetraplex DNA.

Analyses of the Interaction between the Fission Yeast Telomeric DNA and a Series of Mutant Pot1DBD Proteins—To investigate the mechanism underlying the ability of Pot1DBD to unfold the antiparallel tetraplex DNA (Fig. 5B and C), we have studied the interaction between the antiparallel tetraplex of 4G4 and a series of mutant Pot1DBD proteins by EMSA (Fig. 6B). We have also examined the binding affinity of the series of mutant Pot1DBD proteins for the single strand of G2, the minimum DNA sequence for the specific binding of wild-type Pot1DBD (*12, 48, 49*) (Fig. 6C). Point mutations were introduced at S58, D64, K90, Q120, K124 and D125, which are involved in the specific recognition of G2 (Fig. 6A), as judged in a previously reported X-ray crystallographic study of the complex between G2 and Pot1DBD (*49*). The interacting activity of S58A, K90A and D125A with the antiparallel tetraplex of 4G4 (Fig. 6B and data not shown) or the single strand of G2 (Fig. 6C and data not shown) was of similar magnitude to that in the case of the wild-type Pot1DBD (WT) (Table 2). Lower interacting activity with the antiparallel tetraplex of 4G4 (Fig. 6B) or the single strand of G2 (Fig. 6C) was observed for Q120L (Table 2). D64A and K124A completely lost the interacting activity with the antiparallel tetraplex of 4G4 (Fig. 6B and data not shown) or the single strand of G2 (Fig. 6C and data not shown). The binding constants between these mutant Pot1DBDs and the single strand of G2 at 25°C in the same buffer were also measured by isothermal titration calorimetry (ITC). The large binding constants for WT, S58A, K90A and D125A were in the order of $10^7\,M^{-1}$. A binding constant of about $10^6\,M^{-1}$ was obtained for Q120L. Binding constants smaller than $10^5\,M^{-1}$ were observed for D64A and K124A. These binding constants were consistent with the results in Fig. 6C. The details of the ITC experiments will be given elsewhere. These results indicate that the mutant Pot1DBD proteins with the higher binding affinity as to the single strand of G2 have greater ability to interact with the antiparallel tetraplex of 4G4 (Table 2).

Next, the CD spectral change of the antiparallel tetraplex of 4G4 upon the addition of the wild-type or the series of mutant Pot1DBD proteins was measured at 25°C and pH 7.5 in buffer A containing 150 mM NaCl (Fig. 6D). The magnitudes of the decrease in the ellipticity at 295 nm upon the addition of S58A, K90A

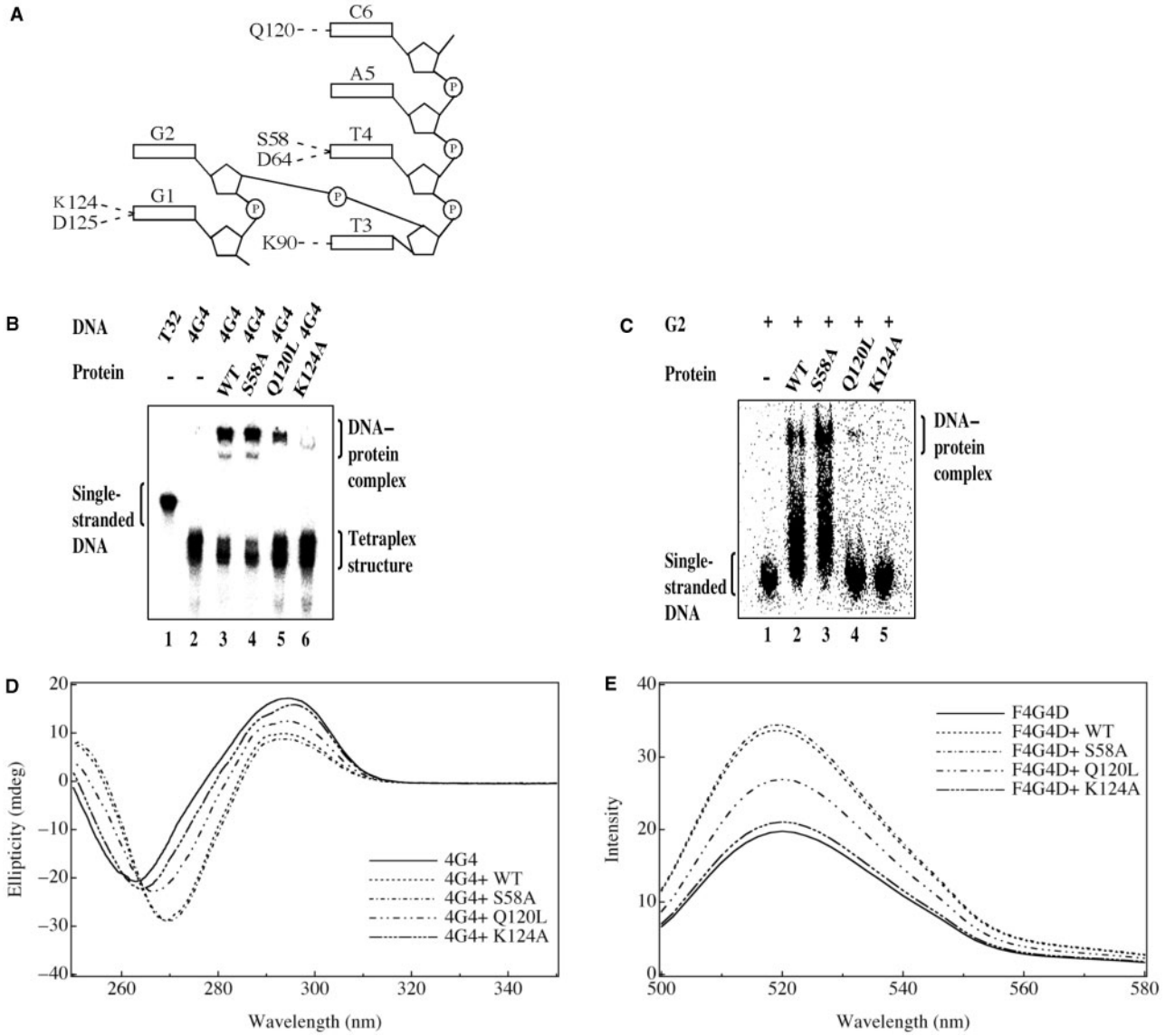

Fig. 6. **Interaction analyses of 4G4 or G2 with the wild-type or a series of mutant Pot1DBD proteins**. (A) A schematic model of the complex between G2 and Pot1DBD. Each amino acid of Pot1DBD binds with each base of G2 by hydrogen-bonding interaction. (B) 20 nM 4G4 at pH 7.5 in buffer A (see 'Materials and Methods') containing 150 mM NaCl was incubated with 1.5 μM wild-type or a mutant Pot1DBD in the same buffer at 25°C for 30 min. A 15% nondenaturing polyacrylamide gel was run in 0.5 × TBE at 10 V/cm and 4°C for 5 h. (C) 500 nM G2 at pH 7.5 in buffer A (see 'Materials and Methods') containing 150 mM NaCl was incubated with 1.5 μM wild-type or a mutant Pot1DBD in the same buffer at 25°C for 30 min. A 10% non-denaturing polyacrylamide gel was run in 0.5 × TBE at 10 V/cm and 4°C for 5 h. (D) 3 μM 4G4 at pH 7.5 in buffer A (see 'Materials and Methods') containing 150 mM NaCl was incubated with a 3 molar excess of the wild-type or a mutant Pot1DBD in the same buffer at 25°C for 60 min before the CD measurements. (**E**) 100 nM F4G4D at pH 7.5 in buffer A (see 'Materials and Methods') containing 150 mM NaCl was incubated in an equimolar ratio with the wild-type or a mutant Pot1DBD in the same buffer at 25°C for 60 min before the fluorescence measurements. The excitation wavelength was 495 nm.

and D125A were similar to that upon the addition of WT (Fig. 6D and data not shown). The decrease in the ellipticity at 295 nm corresponds to a reduction in the amount of the antiparallel tetraplex, as discussed earlier in Fig. 4C and 4D. A smaller magnitude of the decrease in the ellipticity at 295 nm was observed for the addition of Q120L (Fig. 6D). D64A and K124A have little ability to decrease the ellipticity at 295 nm (Fig. 6D and data not shown). These results indicate that the mutant Pot1DBD proteins with the higher binding affinity as to the single strand of G2 have greater ability to reduce the amount of the antiparallel tetraplex by decreasing the ellipticity at 295 nm (Table 2).

In addition, the structural change of F4G4D upon the addition of the wild-type or the series of mutant Pot1DBD proteins was examined by FRET analyses at 25°C and pH 7.5 in buffer A containing 150 mM NaCl (Fig. 6E). The magnitudes of the increase in the intensity

Table 2. **Comparison of properties of the wild-type or a series of mutant Pot1DBD proteins.**

Protein	Affinity to interact with the antiparallel tetraplex[a]	Affinity to interact with the single strand[b]	Ability to decrease the amount of the antiparallel tetraplex[c]	Ability to unfold the antiparallel tetraplex[d]
WT	++	++	++	++
S58A	++	++	++	++
D64A	−	−	−	−
K90A	++	++	++	++
Q120L	+	+	+	+
K124A	−	−	−	−
D125A	++	++	++	++

++, strong activity; +, medium activity; −, weak or no activity; [a]Estimated from Fig. 6B. [b]Estimated from Fig. 6C. [c]Estimated from Fig. 6D. [d]Estimated from Fig. 6E.

at 520 nm upon the addition of S58A, K90A and D125A were similar to that upon the addition of WT (Fig. 6E and data not shown). The increase in the intensity at 520 nm corresponds to the unfolding of the antiparallel tetraplex, as discussed earlier in Fig. 5B and C. A smaller magnitude of the increase in the intensity at 520 nm was observed for the addition of Q120L (Fig. 6E). D64A and K124A have little ability to increase the intensity at 520 nm (Fig. 6E and data not shown). These results indicate that the mutant Pot1DBD proteins with the higher binding affinity as to the single strand of G2 have greater ability to unfold the antiparallel tetraplex by increasing the intensity at 520 nm (Table 2). Combining the results in Fig. 6, we have concluded that the specific binding affinity for the single strand of G2 is strongly correlated with the abilities to reduce the amount of the antiparallel tetraplex and to unfold the antiparallel tetraplex.

DISCUSSION

G2 and G3 only form the unstructured single strand, but G4, G5 and G6 have the ability to form the four-stranded parallel tetraplex in the presence of a cation (Figs 1A and 2A). As the number of consecutive guanines increases, the magnitude of the four-stranded parallel tetraplex increases. This indicates that the increase in the number of consecutive guanines in a single copy may induce the formation of the four-stranded parallel tetraplex. Previous studies revealed that, as the number of consecutive guanines increased in the oligonucleotide sequence d(TG_nT), the thermodynamic stability of the four-stranded parallel tetraplex increased (*56*), which is consistent with the results obtained in this study. Although G4 has the ability to form the four-stranded parallel tetraplex (Figs 1A and 2A), 4G4, i.e. four repeats of G4, forms the antiparalleltetraplex in the presence of a cation (Figs 1B and 2B). This observation shows that the tetraplex topology is dependent on the number of repeats. Previously reported spectroscopic studies in solution showed that a single copy of human telomeric sequence d(TTAGGG) adopted a four-stranded parallel tetraplex (*27*), but that d[$GGG(TTAGGG)_3$, d[$AGGG(TTAGGG)_3$] and $d(TTAGGG)_4$ formed an antiparallel tetraplex (*28–30*), whose dependence on the number of repeats is similar to that observed in this study. Combining these results, we conclude that the tetraplex topology of the fission yeast telomeric DNA is governed by the number of consecutive guanines in a single copy and the number of repeats, which is consistent with the results obtained for the well-characterized telomeric DNA sequences from *Tetrahymena* (*23–27*), *Oxytricha* (*24,* 26), and vertebrates (*27–30*).

Previous studies involving sequence analyses of the fission yeast telomeric DNA (*11, 12*) revealed that the d(GGTTAC) sequence was clearly emerged as the most common motif, and ∽ 20% of the telomeric sequence contains three or four consecutive guanines preceding the TTAC sequence, which is equivalent to G3 or G4 in this study. 4G3 and 4G4, i.e. four copies of G3 and G4, respectively, form the compact parallel or antiparallel tetraplex structure in the presence of a cation (Figs 1B and 2B). Thus, we suggest that at least 20% of the fission yeast telomeric DNA may have the potential to form the compact parallel or antiparallel tetraplex structure, which may inhibit the telomerase-mediated telomeric DNA elongation (*51–53*) discussed subsequently.

The CD spectral change of 4G4 upon the addition of Pot1DBD indicates that Pot1DBD has the ability to decrease the amount of the antiparallel tetraplex DNA (Figs 4C and D). Furthermore, FRET analyses of F4G4D upon the addition of Pot1DBD indicated that Pot1DBD has the ability to unfold the antiparallel tetraplex DNA (Figs 5B and C), which is quite consistent with the ability of Pot1DBD to reduce the amount of the antiparallel tetraplex observed in Figs 4C and D. A decrease in the amount of the antiparallel tetraplex upon the addition of Pot1DBD and unfolding of the antiparallel tetraplex upon the addition of Pot1DBD were also observed both in the presence of 150 mM sodium cation (Figs 4C and 5B) or 30 mM potassium cation (Figs 4D and 5C). The ability to decrease the amount of the antiparallel tetraplex and that to unfold the antiparallel tetraplex may not be significantly influenced by the kind of the coexisting cation. These results suggest that, although Pot1DBD interacts with the antiparallel tetraplex, a stable complex between Pot1DBD and the antiparallel tetraplex cannot be formed. In general, hydrogen bonding and base stacking are important interaction forces for the stable complex formation between DNA-binding proteins and their interacting DNAs (*57, 58*). However, each of the four guanines in the G-quartets of the tetraplex DNA interacts with each of the two adjacent guanines through hydrogen bonding (*17–19*), and each G-quartet is stacked with the neighbouring G-quartets through base stacking (*17–19*). Thus, the interaction with the G-quartets through hydrogen bonding and base stacking from the outside may be difficult, which may result in the inability of Pot1DBD to form a stable complex with the anti-parallel tetraplex. Comparison of the CD spectral changes of 4G4 upon the addition of Pot1DBD (Fig. 4C) and GST (Fig. 4E) indicates that the ability to reduce the amount of the antiparallel tetraplex is specific for Pot1DBD. In addition, the interaction between a series of mutant Pot1DBD proteins and each of the antiparallel

tetraplex of 4G4 or the single-strand of G2 shows that the specific binding affinity for the single strand (Fig. 6C) is strongly correlated with the abilities to reduce the amount of the antiparallel tetraplex (Fig. 6D) and to unfold the antiparallel tetraplex (Fig. 6E). The specific unfolding of 4G4 by Pot1DBD (Fig. 4), and the strong correlation between the binding affinity for the single strand and the ability to unfold the antiparallel tetraplex (Fig. 6) suggest that the antiparallel tetraplex of 4G4 may change into an unstructured single strand after the specific interaction with Pot1DBD, although the exact structure of the complex with Pot1DBD remains to be determined. The higher binding affinity of the wild-type or a part of the mutant Pot1DBDs for the unstructured single strand may decrease the larger amount of the unstructured single strand in the free state. The decrease in the amount of the unstructured single strand in the free state may induce the shift of the equilibrium from the antiparallel tetraplex to the unstructured single strand. This equilibrium shift can cause the unfolding of the antiparallel tetraplex. Such a mechanism may be possible for the unfolding of the antiparallel tetraplex of 4G4 upon the interaction with Pot1DBD (Figs 5B and C).

Previous studies revealed that the antiparallel tetraplex structure did not serve as a good substrate of telomerase (*51–53*). When the fission yeast telomeric DNA forms the antiparallel tetraplex in the presence of a cation (Figs 1B and 2B), the telomerase-mediated telomere elongation may be inhibited. The ability of Pot1DBD to unfold the antiparallel tetraplex (Figs 5B and C) may change the antiparallel tetraplex into the unstructured single strand, which can be a substrate of telomerase. The participation of fission yeast Pot1 in the unfolding of the antiparallel tetraplex may provide a possible means for telomerase-mediated telomere elongation. In fact, overexpression of the fission yeast Pot1 led to modest but significant telomere lengthening *in vivo* (*12, 50*). However, the purified fission yeast Pot1 inhibited telomerase by sequestering the template telomeric DNA *in vitro* (*12*). The stimulation and inhibition of telomerase by the fission yeast Pot1 need not be exclusive, as evidenced by the telomere length regulation in budding yeast. A single-stranded telomeric DNA binding protein, Cdc13, has the ability to denature the tetraplex (*41*) and recruits the catalytic subunit of telomerase Est2 for the telomere elongation by interacting with the telomerase subunit Est1 (*59*). Unidentified fission yeast proteins with the Est1-like activity may be involved in the telomerase-mediated telomere elongation *in vivo*. The unfolding of the antiparallel tetraplex by the fission yeast Pot1 may constitute the basic mechanism for the telomerase-mediated telomere elongation. A previous study revealed that inhibition of telomere elongation activity of telomerase by the tetraplex formation of human telomeric DNA was significantly reduced by the addition of human Pot1 (*53*). Both fission yeast and human may employ a similar strategy of tetraplex unfolding by Pot1 to allow telomerase-mediated telomere elongation.

The present study has demonstrated that the fission yeast telomeric DNA sequences with more consecutive G bases formed a tetraplex structure in the presence of a cation similar to the well-characterized telomeric DNA sequences from *Tetrahymena*, *Oxytricha* and vertebrates. The tetraplex topology is governed by the number of consecutive guanines in a single copy and the number of repeats. The present study has also demonstrated that the antiparallel tetraplex structure became unfolded upon the interaction with Pot1DBD. The study of the interaction with the series of mutant Pot1DBD proteins revealed that the ability to unfold the antiparallel tetraplex was strongly correlated with the specific binding affinity for the single strand. The result suggests a possible unfolding mechanism that the decrease in the amount of the single strand in the free state upon the single strand-Pot1DBD complex formation may induce a shift in the equilibrium from the antiparallel tetraplex to the single strand, which may cause the unfolding of the antiparallel tetraplex. Considering that the antiparallel tetraplex is known to inhibit telomerase-mediated telomere elongation, we conclude that the ability of fission yeast Pot1 to unfold the antiparallel tetraplex of the telomeric DNA is required for regulation of telomerase-mediated telomere elongation. Our results certainly support the idea that unfolding of the tetraplex by telomeric DNA binding proteins could be a key strategy for regulation of telomerase-mediated telomere elongation and may eventually lead to progress in the understanding of telomere length regulation mechanism by telomere-binding proteins and telomerase.

We thank Dr Naoshi Dohmae for measurement of the mass spectra of the wild-type and the series of mutant Pot1DBD proteins. This research was supported in part by Grants-in-Aid for Scientific Research (B) (16390083) and Priority Areas (17012022 and 17053027) from the Ministry of Education, Science, Sports and Culture of Japan.

REFERENCES

1. Vega, L.R., Mateyak, M.K., and Zakian, V.A. (2003) Getting to the end: telomerase access in yeast and humans. *Nat Rev Mol Cell Biol* **4**, 948–959
2. Cech, T.R. (2004) Beginning to understand the end of the chromosome. *Cell* **116**, 273–279
3. Smogorzewska, A. and de Lange, T. (2004) Regulation of telomerase by telomeric proteins. *Annu Rev Biochem* **73**, 177–208
4. Blackburn, E.H. (2005) Telomeres and telomerase: their mechanisms of action and the effects of altering their functions. *FEBS Lett* **579**, 859–862
5. de Lange, T. (2005) Shelterin: the protein complex that shapes and safeguards human telomeres. *Genes Dev* **19**, 2100–2110
6. Blackburn, E.H. and Gall, J.G. (1978) A tandemly repeated sequence at the termini of the extrachromosomal ribosomal RNA genes in *Tetrahymena*. *J Mol Biol* **120**, 33–53
7. Oka, Y., Shiota, S., Nakai, S. *et al.* (1980) Inverted terminal repeat sequence in the macronuclear DNA of Stylonychia pustulata. *Gene* **10**, 301–306
8. Klobutcher, L.A., Swanton, M.T., Donini, P. *et al.* (1981) All gene-sized DNA molecules in four species of hypotrichs have the same terminal sequence and an unusual 3' terminus. *Proc Natl Acad Sci USA* **78**, 3015–3019
9. Moyzis, R.K., Buckingham, J.M., Cram, L.S. *et al.* (1988) A highly conserved repetitive DNA sequence, (TTAGGG)n,

present at the telomeres of human chromosomes. *Proc Natl Acad Sci USA* **85**, 6622–6626
10. Shampay, J., Szostak, J.W., and Blackburn, E.H. (1984) DNA sequences of telomeres maintained in yeast. *Nature* **310**, 154–157
11. Sugawara, N.F. (1988) *DNA Sequences at the Telomeres of the Fission Yeast* S. pombe Harvard University, Cambridge, MA
12. Trujillo, K.M., Bunch, J.T., and Baumann, P. (2005) Extended DNA binding site in Pot1 broadens sequence specificity to allow recognition of heterogeneous fission yeast telomeres. *J Biol Chem* **280**, 9119–9128
13. Harley, C.B., Futcher, A.B., and Greider, C.W. (1990) Telomeres shorten during ageing of human fibroblasts. *Nature* **345**, 458–460
14. Hastie, N.D., Dempster, M., Dunlop, M.G. *et al.* (1990) Telomere reduction in human colorectal carcinoma and with ageing. *Nature* **346**, 866–868
15. de Lange, T., Shiue, L., Myers, R.M. *et al.* (1990) Structure and variability of human chromosome ends. *Mol Cell Biol* **10**, 518–527
16. Levy, M.Z., Allsopp, R.C., Futcher, A.B. *et al.* (1992) Telomere end-replication problem and cell aging. *J Mol Biol* **225**, 951–960
17. Mills, M., Lacroix, L., Arimondo, P.B. *et al.* (2002) Unusual DNA conformations: implications for telomeres. *Curr Med Chem Anticancer Agents* **2**, 627–644
18. Neidle, S. and Parkinson, G.N. (2003) The structure of telomeric DNA. *Curr Opin Struct Biol* **13**, 275–283
19. Ghosal, G. and Muniyappa, K. (2006) Hoogsteen base-pairing revisited: resolving a role in normal biological processes and human diseases. *Biochem Biophys Res Commun* **343**, 1–7
20. Arnott, S., Chandrasekaran, R., and Marttila, C.M. (1974) Structures for polyinosinic acid and polyguanylic acid. *Biochem J* **141**, 537–543
21. Zimmerman, S.B., Cohen, G.H., and Davies, D.R. (1975) X-ray fiber diffraction and model-building study of polyguanylic acid and polyinosinic acid. *J Mol Biol* **92**, 181–192
22. Sen, D. and Gilbert, W. (1988) Formation of parallel four-stranded complexes by guanine-rich motifs in DNA and its implications for meiosis. *Nature* **334**, 364–366
23. Sundquist, W.I. and Klug, A. (1989) Telomeric DNA dimerizes by formation of guanine tetrads between hairpin loops. *Nature* **342**, 825–829
24. Williamson, J.R., Raghuraman, M.K., and Cech, T.R. (1989) Monovalent cation-induced structure of telomeric DNA: the G-quartet model. *Cell* **59**, 871–880
25. Hardin, C.C., Henderson, E., Watson, T. *et al.* (1991) Monovalent cation induced structural transitions in telomeric DNAs: G-DNA folding intermediates. *Biochemistry* **30**, 4460–4472
26. Balagurumoorthy, P., Brahmachari, S.K., Mohanty, D. *et al.* (1992) Hairpin and parallel quartet structures for telomeric sequences. *Nucleic Acids Res* **20**, 4061–4067
27. Wang, Y. and Patel, D.J. (1992) Guanine residues in d(T2AG3) and d(T2G4) form parallel-stranded potassium cation stabilized G-quadruplexes with anti glycosidic torsion angles in solution. *Biochemistry* **31**, 8112–8119
28. Wang, Y. and Patel, D.J. (1993) Solution structure of the human telomeric repeat d[AG3(T2AG3)3] G-tetraplex. *Structure* **1**, 263–282
29. Balagurumoorthy, P. and Brahmachari, S.K. (1994) Structure and stability of human telomeric sequence. *J Biol Chem* **269**, 21858–21869
30. Vorlickova, M., Chladkova, J., Kejnovska, I. *et al.* (2005) Guanine tetraplex topology of human telomere DNA is governed by the number of (TTAGGG) repeats. *Nucleic Acids Res* **33**, 5851–5860
31. Arthanari, H. and Bolton, P.H. (2001) Functional and dysfunctional roles of quadruplex DNA in cells. *Chem Biol* **8**, 221–230
32. Walsh, K. and Gualberto, A. (1992) MyoD binds to the guanine tetrad nucleic acid structure. *J Biol Chem* **267**, 13714–13718
33. Weisman-Shomer, P. and Fry, M. (1993) QUAD, a protein from hepatocyte chromatin that binds selectively to guanine-rich quadruplex DNA. *J Biol Chem* **268**, 3306–3312
34. Schierer, T. and Henderson, E. (1994) A protein from Tetrahymena thermophila that specifically binds parallel-stranded G4-DNA. *Biochemistry* **33**, 2240–2246
35. Frantz, J.D. and Gilbert, W. (1995) A novel yeast gene product, G4p1, with a specific affinity for quadruplex nucleic acids. *J Biol Chem* **270**, 20692–20697
36. Frantz, J.D. and Gilbert, W. (1995) A yeast gene product, G4p2, with a specific affinity for quadruplex nucleic acids. *J Biol Chem* **270**, 9413–9419
37. Sarig, G., Weisman-Shomer, P., Erlitzki, R. *et al.* (1997) Purification and characterization of qTBP42, a new single-stranded and quadruplex telomeric DNA-binding protein from rat hepatocytes. *J Biol Chem* **272**, 4474–4482
38. Erlitzki, R. and Fry, M. (1997) Sequence-specific binding protein of single-stranded and unimolecular quadruplex telomeric DNA from rat hepatocytes. *J Biol Chem* **272**, 15881–15890
39. Uliel, L., Weisman-Shomer, P., Oren-Jazan, H. *et al.* (2000) Human Ku antigen tightly binds and stabilizes a tetrahelical form of the Fragile X syndrome d(CGG)n expanded sequence. *J Biol Chem* **275**, 33134–33141
40. Weisman-Shomer, P., Naot, Y., and Fry, M. (2000) Tetrahelical forms of the fragile X syndrome expanded sequence d(CGG)(n) are destabilized by two heterogeneous nuclear ribonucleoprotein-related telomeric DNA-binding proteins. *J Biol Chem* **275**, 2231–2238
41. Lin, Y. C., Shih, J. W., Hsu, C. L. *et al.* (2001) Binding and partial denaturing of G-quartet DNA by Cdc13p of *Saccharomyces cerevisiae*. *J Biol Chem* **276**, 47671–47674
42. Fukuda, H., Katahira, M., Tsuchiya, N. *et al.* (2002) Unfolding of quadruplex structure in the G-rich strand of the minisatellite repeat by the binding protein UP1. *Proc Natl Acad Sci U S A* **99**, 12685–12690
43. Weisman-Shomer, P., Cohen, E., and Fry, M. (2002) Distinct domains in the CArG-box binding factor A destabilize tetraplex forms of the fragile X expanded sequence d(CGG)n. *Nucleic Acids Res* **30**, 3672–3681
44. Khateb, S., Weisman-Shomer, P., Hershco, I. *et al.* (2004) Destabilization of tetraplex structures of the fragile X repeat sequence (CGG)n is mediated by homolog-conserved domains in three members of the hnRNP family. *Nucleic Acids Res* **32**, 4145–4154
45. Kankia, B.I., Barany, G., and Musier-Forsyth, K. (2005) Unfolding of DNA quadruplexes induced by HIV-1 nucleocapsid protein. *Nucleic Acids Res* **33**, 4395–4403
46. Enokizono, Y., Konishi, Y., Nagata, K. *et al.* (2005) Structure of hnRNP D complexed with single-stranded telomere DNA and unfolding of the quadruplex by heterogeneous nuclear ribonucleoprotein D. *J Biol Chem* **280**, 18862–18870
47. Baumann, P. and Cech, T.R. (2001) Pot1, the putative telomere end-binding protein in fission yeast and humans. *Science* **292**, 1171–1175
48. Lei, M., Baumann, P., and Cech, T.R. (2002) Cooperative binding of single-stranded telomeric DNA by the Pot1 protein of *Schizosaccharomyces pombe*. *Biochemistry* **41**, 14560–14568
49. Lei, M., Podell, E.R., Baumann, P. *et al.* (2003) DNA self-recognition in the structure of Pot1 bound to telomeric single-stranded DNA. *Nature* **426**, 198–203
50. Bunch, J.T., Bae, N.S., Leonardi, J. *et al.* (2005) Distinct requirements for Pot1 in limiting telomere length and maintaining chromosome stability. *Mol Cell Biol* **25**, 5567–5578

51. Zahler, A.M., Williamson, J.R., Cech, T.R. *et al.* (1991) Inhibition of telomerase by G-quartet DNA structures. *Nature* **350**, 718–720
52. Fletcher, T.M., Sun, D., Salazar, M. *et al.* (1998) Effect of DNA secondary structure on human telomerase activity. *Biochemistry* **37**, 5536–5541
53. Zaug, A.J., Podell, E.R., and Cech, T.R. (2005) Human POT1 disrupts telomeric G-quadruplexes allowing telomerase extension *in vitro*. *Proc Natl Acad Sci U S A* **102**, 10864–10869
54. Mergny, J.L. (1999) Fluorescence energy transfer as a probe for tetraplex formation: the i-motif. *Biochemistry* **38**, 1573–1581
55. Mergny, J.L. and Maurizot, J.C. (2001) Fluorescence resonance energy transfer as a probe for G-quartet formation by a telomeric repeat. *Chembiochem* **2**, 124–132
56. Petraccone, L., Erra, E., Duro, I. *et al.* (2005) Relative stability of quadruplexes containing different number of G-tetrads. *Nucleosides Nucleotides Nucleic Acids* **24**, 757–760
57. Lamoureux, J.S., Maynes, J.T., and Glover, J.N. (2004) Recognition of 5'-YpG-3' sequences by coupled stacking/hydrogen bonding interactions with amino acid residues. *J Mol Biol* **335**, 399–408
58. Sarai, A. and Kono, H. (2005) Protein-DNA recognition patterns and predictions. *Annu Rev Biophys Biomol Struct* **34**, 379–398
59. Pennock, E., Buckley, K., and Lundblad, V. (2001) Cdc13 delivers separate complexes to the telomere for end protection and replication. *Cell* **104**, 387–396